© 2012 Triveni Enterprises
Vikas Nagar, Lucknow, INDIA
editor@jeb.co.in
Full paper available on: www.jeb.co.in

J. Environ. Biol.
33, 475-485 (2012)
ISSN: 0254-8704
CODEN: JEBIDP

# Analysis of the climate variability on Lake Nasser evaporation based on the Bowen ratio energy budget method

**Author Details**

**Mohamed Elsawwaf** (*Corresponding author*)
Hydraulics Laboratory, Department of Civil Engineering, Katholieke Universiteit Leuven, Kasteelpark Arenberg 40, 3001 Heverlee
Water Resources Research Institute, National Water Research Center, El-Qanater El-Khiria. 13621, Egypt.
e-mail: ahmed_karem40@yahoo.com

**Patrick Willems**
Hydraulics Laboratory, Department of Civil Engineering, Katholieke Universiteit Leuven, Kasteelpark Arenberg 40, 3001 Heverlee, Belgium

**Publication Data**

*Paper received:*
25 October 2010

*Revised received:*
05 July 2011

*Accepted:*
30 July 2011

**Abstract**

Variations in lake evaporation have a significant impact on the energy and water budgets of lakes. Understanding these variations and the role of climate is important for water resources management as well as predicting future changes in lake hydrology as a result of climate change. This study presents a comprehensive, 10-year analysis of seasonal, intraseasonal, and interannual variations in lake evaporation for Lake Nasser in South Egypt. Meteorological and lake temperature measurements were collected from an instrumented platform (Raft floating weather station) at 2 km upstream of the Aswan High Dam. In addition to that, radiation measurements at three locations on the lake: Allaqi, Abusembel and Arqeen (respectively at 75, 280 and 350 km upstream of the Aswan High Dam) are used. The data were analyzed over 14-day periods from 1995 to 2004 to provide bi-weekly energy budget estimates of evaporation rate. The mean evaporation rate for lake Nasser over the study period was 5.88 mm day$^{-1}$, with a coefficient of variation of 63%. Considerable variability in evaporation rates was found on a wide range of timescales, with seasonal changes having the highest coefficient of variation (32%), followed by the intraseasonal (28%) and interannual timescales (11.6%; for summer means). Intraseasonal changes in evaporation were primarily associated with synoptic weather variations, with high evaporation events tending to occur during incursions of cold, dry air (due, in part, to the thermal lag between air and lake temperatures). Seasonal variations in evaporation were largely driven by temperature and net energy advection, but are out-of-phase with changes in wind speed. On interannual timescales, changes in summer evaporation rates were strongly associated with changes in net energy advection and showed only moderate connections to variations in temperature or humidity.

**Key words**

Lake Nasser, Energy budget, Climate variability, Bowen ratio energy budget (BREB)

## Introduction

Lakes and reservoirs provide a valuable water resource that is important for irrigation, fishing and recreation, drinking water, aquatic ecosystems, transportation and commerce, and hydropower. The availability and quality of freshwater is, in turn, closely tied to variations in climate as well as direct human influences (*e.g.* Lenters *et al*., 2005; Schindler, 2001). One of the most significant and broadly impacting effects of climate variability on lakes are changes in water level. Such changes reflect an alteration of the lake water balance, which can result from changes in: (1) precipitation over the lake and surrounding watershed, (2) land surface evapotranspiration and snowmelt (and associated surface runoff and/or groundwater flow), and/or (3) direct evaporation from the lake surface. It is crucial for water resource management, therefore, the effects of climate variability on each of these hydrologic processes be well understood. Lake evaporation is somewhat unique in the sense that it is influenced not only by climate, but also by characteristics of the lake itself (*e.g.* depth, area, color/clarity *etc.*) (Lenters *et al.*, 2005). Furthermore, evaporation plays an important role not only in the water budget of a lake, but also in the energy budget. This introduces additional

complexity through changes in water temperature and vertical mixing; effects which actually feedback onto evaporation itself. Even measuring evaporation accurately (within 10%) is a difficult task without significant investment in instrumentation and data processing (Lenters *et al.*, 2005; Winter, 1981; Winter *et al.*, 2003). These practical and theoretical considerations impose significant challenges for lake evaporation studies (both observational and modeling), especially when considering long time periods and/or large lakes or regions (with varying climatic and lake characteristics). Despite these challenges, it is critical that accurate, long-term studies of lake evaporation be maintained in order to better understand variations in evaporation as well as the role of climate and potential impacts of climate change.

Lake Nasser is a 6540 $km^2$ lake located in the lower Nile river basin at the border between Egypt and Sudan (Fig. 1). The lake was created during late 1960's to 1970's with the construction of Aswan high dam (AHD) upstream of the old Aswan dam, about 5 km south of Aswan city. AHD is a multi-purpose storage reservoir to provide adequate summer water, hydropower, flood protection and improved river navigation. The reservoir reached its highest level, 182 m a.m.s.l during the water year 1999-2000. At that level, the reservoir lies between latitudes 23°58'N and 20°27'N and longitudes 30°07'E and 33°15'E, with a length of about 500, 350 km of which lies in Egypt and 150 km in Sudan. The maximum width is about 60 km, the average width 10 km, the maximum depth about 90 m and the average depth 25 m. The total capacity of the reservoir is $162.3x10^9$ $m^3$ at the level 182 m a.m.s.l (Sadek *et al.*, 1997; Omar and El Bakry, 1981). The Ministry of Water Resources and Irrigation in Egypt for many years adopted the figure of 7.54 mm $d^{-1}$ as the annual mean evaporation (Whittington and Guariso, 1983). The maximum, in June, is 10.8 mm $d^{-1}$, and the minimum, in December, is 3.95 mm $d^{-1}$, when the lake level is at 160 m a.m.s.l. (Sadek *et al.*, 1997).

Previous estimates of average annual evaporation from Lake Nasser fall in the range from 1.7 m to 2.9 m (Elsawwaf *et al.*, 2010a). Recently, Elsawwaf *et al.* (2010a) presented an update of these estimates, making use of the Bowen ratio energy budget method (BREB) as a standard method, using 10 years of local meteorological and hydrological data collected from three instrumented platforms along Lake Nasser. The results of the BREB method showed that there is no significant difference between the evaporation rates at the three locations. The obtained evaporation values from the BREB method compared well with the values from six conventional evaporation quantification methods. Most of the previous studies of evaporation estimates from Lake Nasser applied these conventional methods except Omar and El-Bakry (1981) and Sadek *et al.* (1997), who made use of energy budget method but with very limited data. Previous estimates of evaporation relied on data from ground stations except the Elsawwaf et al. (2010a) study.

The present study of the climate variability on Lake Nasser evaporation was designed to be similar to this conducted for Sparkling lake, Northern Wisconsin (USA) (Lenters *et al.*, 2005). The goal of the current study was to provide a comprehensive, quantitative, energy-budget analysis of interannual, seasonal, and intraseasonal variations in lake evaporation, as well as the climatic mechanisms responsible for the variations. Our study covered 10 full open-water seasons, and special care was taken to ensure that the energy-budget periods were same from year to year so that variations in evaporation rate can be appropriately analyzed for each of the time scales under consideration. This report provides a complete description of the first set of data to come out of this study, as well as a detailed methodology, extensive error analysis, and thorough discussion of the results and conclusions of the study.

## Materials and Methods

**Data sources:** In this study, climatological data have been considered from the instrumented platform (floating weather station) at Raft (2 km upstream AHD). It is one of the weather stations operated by the AHD Authority, Egypt. Lake water temperatures at different depths, air temperature over the lake, wind speed and direction, relative humidity at different heights over the lake, and barometric data (atmospheric pressure) were available. The net radiation data were collected at three floating weather stations on the lake: at Allaqi, Abusembel and Arqeen (respectively at 75, 280 and 330 km upstream of the AHD). Water temperature surveys were moreover available at two other locations: Amda Temple and Toshka (respectively 185 and 240 km upstream of the AHD). Fig. 1 shows all meteorological stations inside Lake Nasser.

Apart from lake surveys, all measurements were made at 1 hr intervals and averaged to daily. Further averaging to 14 day running means was performed to be consistent with the temperature surveys at Amda temple and Toshka, which were biweekly, as well as to provide a robust timescale for application of the energy budget technique. The 14 day means were centred on day 8, with days 1 and 15 weighted by 50% to result in a 14 day average. The days and 14 day periods had a beginning and ending time on 12:00 local time.

Elsawwaf *et al.* (2010a) analyzed the quality of the 10 years of data (1995-2004) at Raft station. They analyzed the amount of missing data and the presence of outliers. The result of that analysis showed that the air temperature ($T_a$) values at Raft station is subject to high uncertainty. The calculated standard deviation of the evaporation error at Raft station using the BREB method was 0.62 mm $day^{-1}$. The same 10 yr of data were used in this study.

**Bowen ratio energy budget (BREB) method:** When the BREB method is applied to a system, the energy used for evaporation is calculated as the residual energy after all other energy fluxes are summed. The volume of water evaporated is calculated by dividing the residual energy used for evaporation by the latent heat of evaporation and the density of water. The general form of energy budget equation (*e.g.* Lee and Swancar, 1996; Lenters *et al.*,

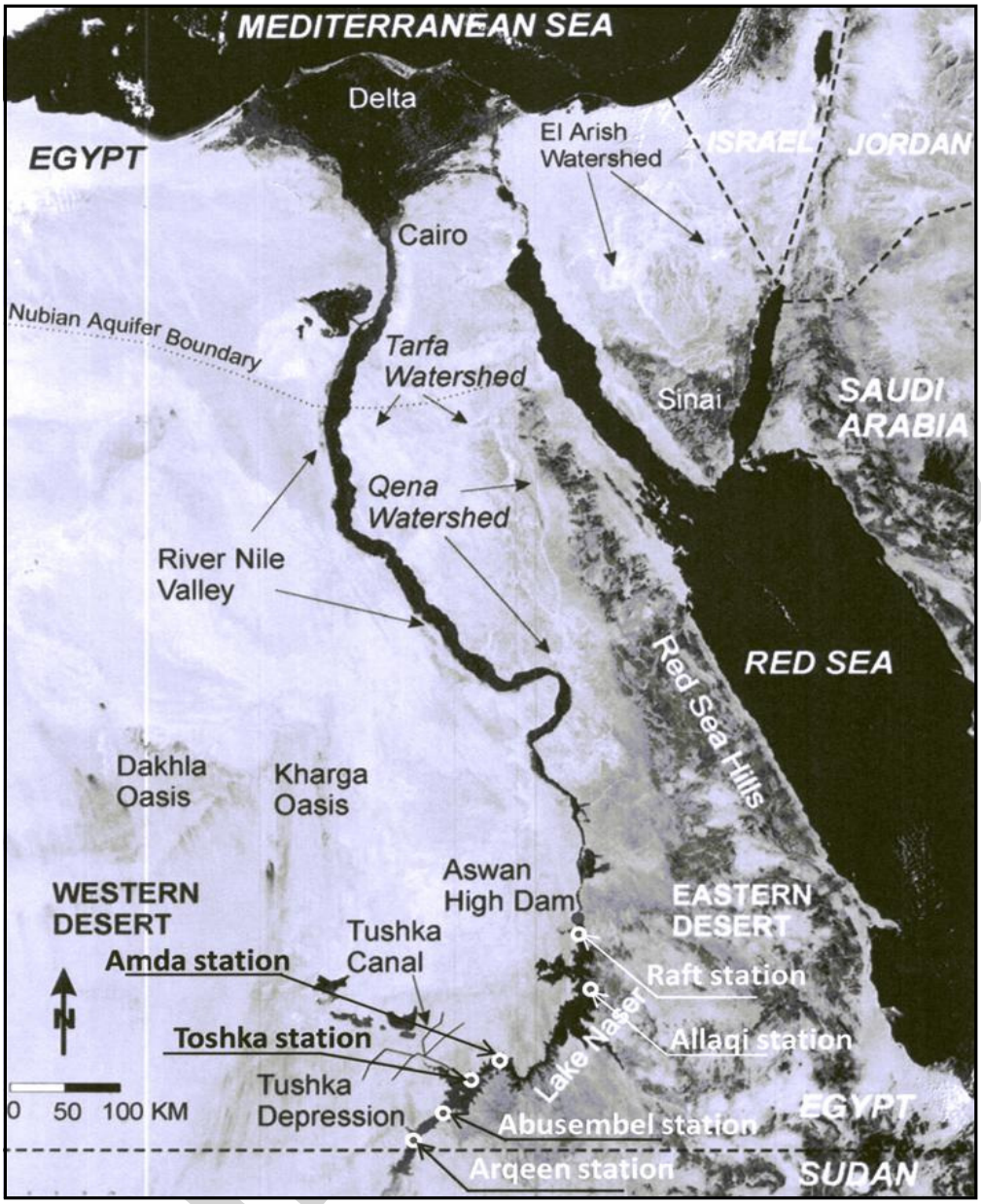


**Fig. 1:** Moderate resolution imaging spectroradiometer satellite image acquired on February 19, 2000, showing the floating weather stations and the general features of the Lake Nasser area in Egypt

2005; Rosenberry, 2007) is

$$Q_s - Q_r + Q_a - Q_{ar} - Q_{bs} + Q_v - Q_w - Q_e - Q_h = Q_x \quad (1)$$

where $Q_s$ is the incident shortwave solar radiation, $Q_r$ is the reflected shortwave solar radiation, $Q_a$ is the incident longwave radiation from the atmosphere, $Q_{ar}$ is the reflected longwave radiation, $Q_{bs}$ is the longwave radiation emitted by the lake, $Q_v$ is the net energy advected by streamflow, groundwater and precipitation, $Q_w$ is the energy advected by evaporating water, $Q_e$ is the energy used for evaporation, $Q_h$ is the energy conducted and convected from the lake to the atmosphere as sensible heat and $Q_x$ is the change in stored energy. All units are in W $m^{-2}$.

The net radiation ($Q_n$) was measured directly and can be expressed as :

$$Q_n = Q_s - Q_r + Q_a - Q_{ar} - Q_{bs} \quad (2)$$

The $Q_n$ was measured at Raft station (during October-December, 2004 and February, 2005 - October, 2006). Elsawwaf *et al.* (2010a) used the empirical equations described by the FAO-56 procedure (Allen *et al.*, 1998) to fill gaps in data or unreliable data. They found that this method provides $Q_n$ estimates, which are in good agreement with the observations ($R^2$=0.82).

$Q_v$ is considered one of the most important terms of the energy budget equation of Lake Nasser. The $Q_v$ parameter was calculated from the daily surface water in- and outflows to and from the lake and temperatures using the following formula:

$$Q_v = \frac{c\rho q_i(T_i - T_b) - c\rho q_o(T_o - T_b)}{A} \quad (3)$$

where $q_i$ is the inflow to the lake ($m^3$), $q_o$ the outflow from the lake ($m^3$), $T_i$ the daily average temperature of water inflow (°C), $T_o$ the daily average temperature of water outflow (°C) and A the daily surface lake area ($m^2$). Equation 3 was multiplied by 11.6 x $10^{-6}$ to obtain a unit of W $m^{-2}$ for $Q_v$. Inflow from upper Nile catchments is assumed to be the only source of advected heat to Lake Nasser. In Eq. 3, the inflow is based on the measured flow at Dongola station (about 280 km south of the entrance of the lake) while the outflow from the lake was based on the flow data at the AHD gates. The temperature of the inflowing water was obtained from the daily measured lake water surface temperature at Arqeen station (331 km upstream of the AHD). The water temperature of the outflow released from the AHD gates was estimated using the measured water temperature at 50 m depth at Raft station. This deepest observation depth was taken because the water was flowing out at the bottom of the AHD at a level of 121.30 m a.m.s.l.

The $Q_x$ parameter is an essential component of the energy budget because the large specific heat capacity of water allows even a small lake to store and exchange large amounts of energy. Daily stored heat was computed from the thermocouples based hourly water temperature measurements at depths 0, 2, 5, 10, 15, 20, 30, 40 and 50 m. Since the temperature varies with depth in the lake, the stored heat was numerically integrated using increments of volume for each of the nine layers in which the temperature was measured and assumed constant:

$$Q_x = \frac{c\rho_w \sum_{i=1}^{n}(T_{2i} - T_b)\Delta V_{2i} - c\rho_w \sum_{i=1}^{m}(T_{1i} - T_b)\Delta V_{1i}}{A} \quad (4)$$

where 1and 2 refers to conditions at the beginning and the end of the period, n and m to the number of water layers, $T_{1i}$ is the temperature of layer (water body) i at the beginning of the period (°C), $T_{2i}$ the temperature of layer (water body) i at the end of the period (°C), $V_{1i}$ the volume of water in the layer i at the beginning of the period ($m^3$), and $V_{2i}$ the volume of water in the layer i at the end of the day ($m^3$). As in Eq. 3, the result of Eq. 4 was multiplied by 11.6 x $10^{-6}$ to convert the unit of $Q_x$ to W $m^{-2}$. It is noteworthy that the net increase or decrease in $Q_x$ equals 22.97 W $m^{-2}$ over the entire period at Raft station. This value should be close to zero when using the average data.

Three types of energy flux-conduction of heat through the lake bottom, the conversion due to chemical and biological processes, and the conversion of kinetic energy to heat energy were assumed to be negligible. Energy advected by evaporating water can be computed as:

$$Q_w = c\rho E_{EB}(T_0 - T_b) \times 86.4 \times 10^6 \quad (5)$$

where c is the specific heat of water (4,186 J $kg^{-1}$ °$C^{-1}$), ρ is the density of evaporating water (998 kg $m^{-3}$), $E_{EB}$ the volume of evaporating water by the BREB method (mm $day^{-1}$), $T_0$ the lake water surface temperature (°C) and $T_b$ the reference base temperature (0°C).

The $Q_e$ also can be expressed as:

$$Q_e = \rho E_{EB} L \times 86.4 \times 10^6 \quad (6)$$

The multiplier 86.4 x $10^6$ in the Eqs. 5 and 6 is to use $E_{EB}$ with mm $day^{-1}$.

$Q_h$, and $Q_e$ are combined using a theoretical relation derived by the Bowen ratio (BR):

$$BR = Q_h/Q_e = \frac{c_{pa}P_a}{0.622L}\frac{T_0 - T_a}{e_0 - e_a} \quad (7)$$

where $c_{pa}$ is the specific heat of air at constant pressure (1011 J $kg^{-1}$°$C^{-1}$), $P_a$ the atmospheric pressure at the water level of the lake (Pa), $e_0$ the saturation vapor pressure at the water surface temperature (Pa), $e_a$ the vapor pressure at 2 m above the lake (Pa) and L the latent heat of vaporization (J $kg^{-1}$).

The final BREB equation then is stated as:

$$E_{EB} = \frac{Q_n + Q_v - Q_x}{\rho[L(1 + BR) + c(T_0 - T_b)]} \times 8.64 \times 10^7 \quad (8)$$

The multiplier 8.64x$10^7$ used in Eq. 8 aims to convert the output to mm $d^{-1}$.

## Results and Discussion

**Evaporation rate and mean energy budget:** Fig. 2 shows the 14 day running mean evaporation rate for 1995-2004 as calculated from Eq. (8). A wide range of variability was revealed, from a maximum of 18.50 mm $d^{-1}$ during 9-23 September, 1998 to a minimum of 0.21 mm $d^{-1}$ during 23 April – 5 May, 1998. The mean evaporation rate (Table 1) for the entire period was 167.4 W $m^{-2}$ (5.86 mm $day^{-1}$), with a standard deviation of 42.93 W $m^{-2}$ (1.50 mm $day^{-1}$). This evaporative heat flux combined with the net energy advected by streamflow of 17.7 W $m^{-2}$ and the change in stored energy of 2.44 W $m^{-2}$ to produce a net evaporation of 167.4 W $m^{-2}$ at the lake surface and an overall BR of -0.04. Most of the evaporated surface was balanced by net radiation (148.2 W $m^{-2}$), which, in turn, was dominated by absorbed solar radiation.

The variations in evaporation rate shown in Fig. 2 are found to span a broad range of temporal scales. For example, a seasonal cycle was clearly evident, with low evaporation rates in

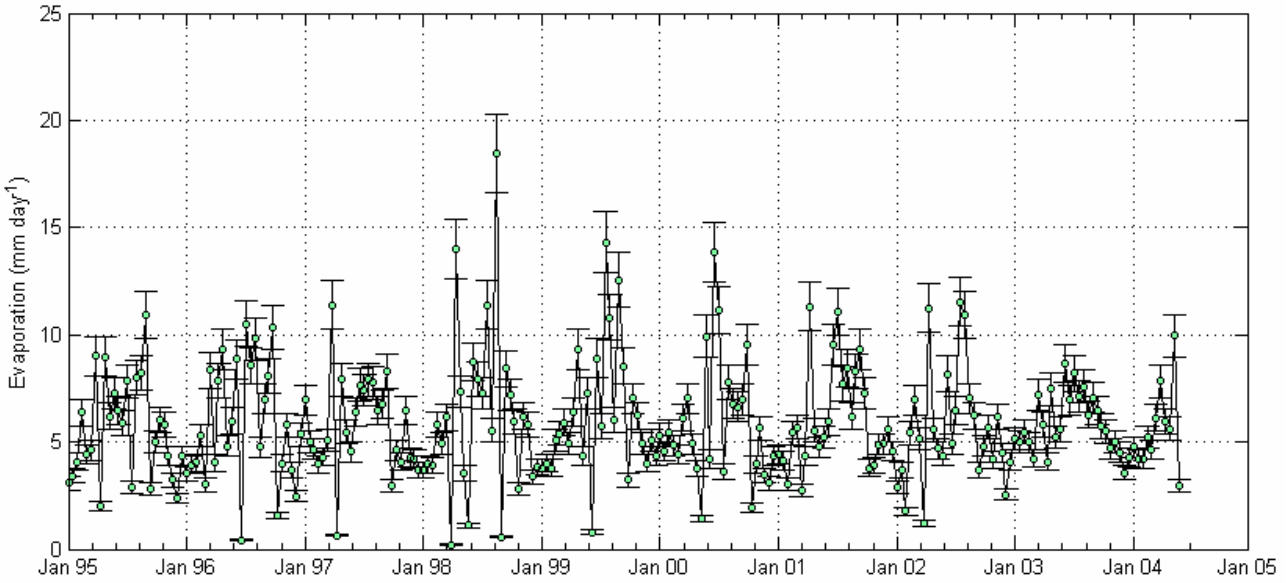


**Fig. 2:** Lake Nasser evaporation rates for bi weekly running means, calculated using Eq. 8. Error bars indicate the estimated standard deviation error (≈9.3% of its mean value) as calculated by Elsawwaf *et al*. (2010b)

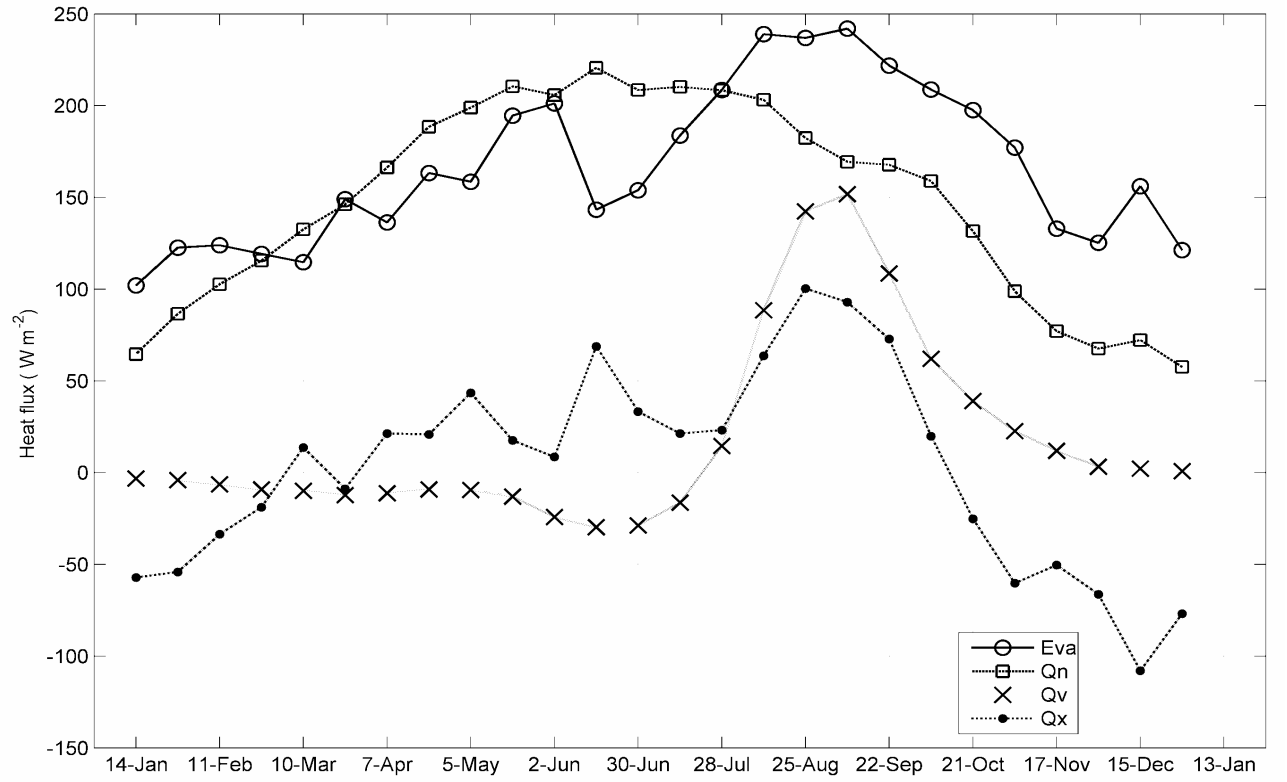


**Fig. 3:** Mean energy budget for Lake Nasser for each of the 26 biweekly periods (averaged over the number of years indicated in Table 1). Heat flux components include $Q_n$, $Q_x$ and $Q_v$

winter and spring followed by high evaporation in summer and low values in autumn. Interannual variations were also evident with high evaporation rates in 1998 and 1999 and low amounts in 2003. Finally, significant short-term variations in evaporation (on roughly 14 to 30 day timescales) are seen in Fig. 2 as well. Particularly dramatic examples of this occurred in 1998 and 1999, when evaporation rates changed by up to a factor of nine in as little as two weeks. These strong intraseasonal variations

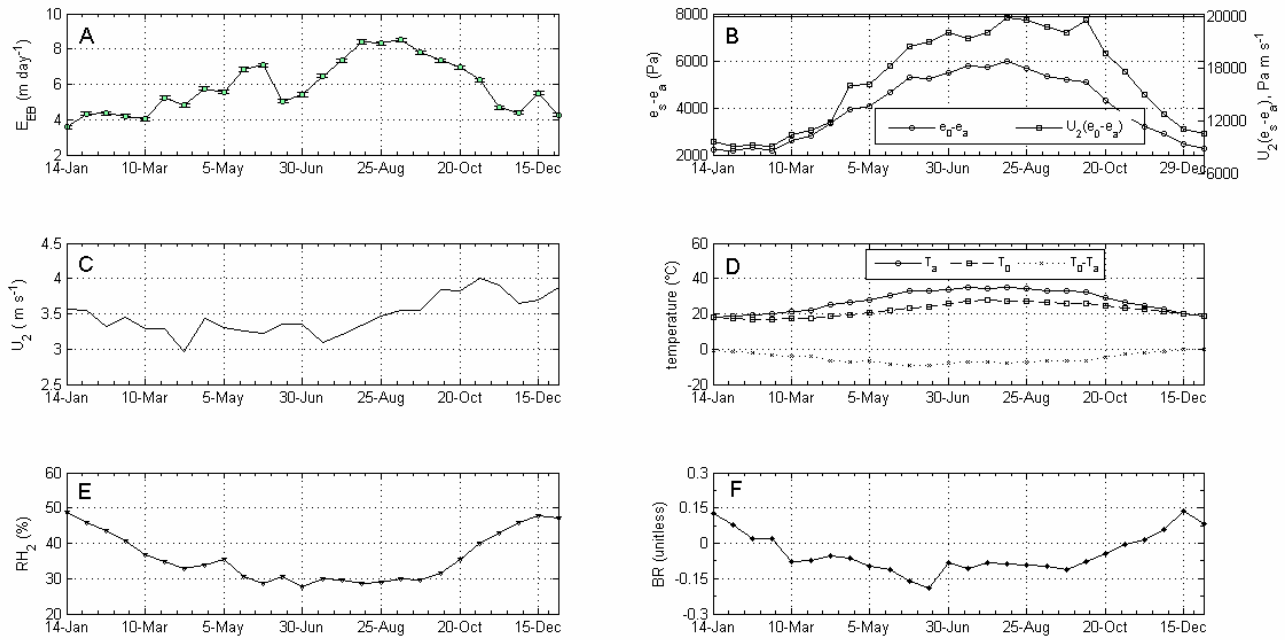


**Fig. 4:** Mean seasonal values of atmospheric and limnological variables for Lake Nasser. Quantities include (A) $E_{EB}$, (B) $e_0$-$e_a$ and $U_2(e_0-e_a)$ (C) $U_2$, (D) $T_0$, $T_a$ and $T_0$-$T_a$ (E) $RH_2$ and (F) BR. Error bars for $E_{EB}$ indicate the estimated standard deviation error as calculated by Elsawwaf *et al.* (2010a,b)

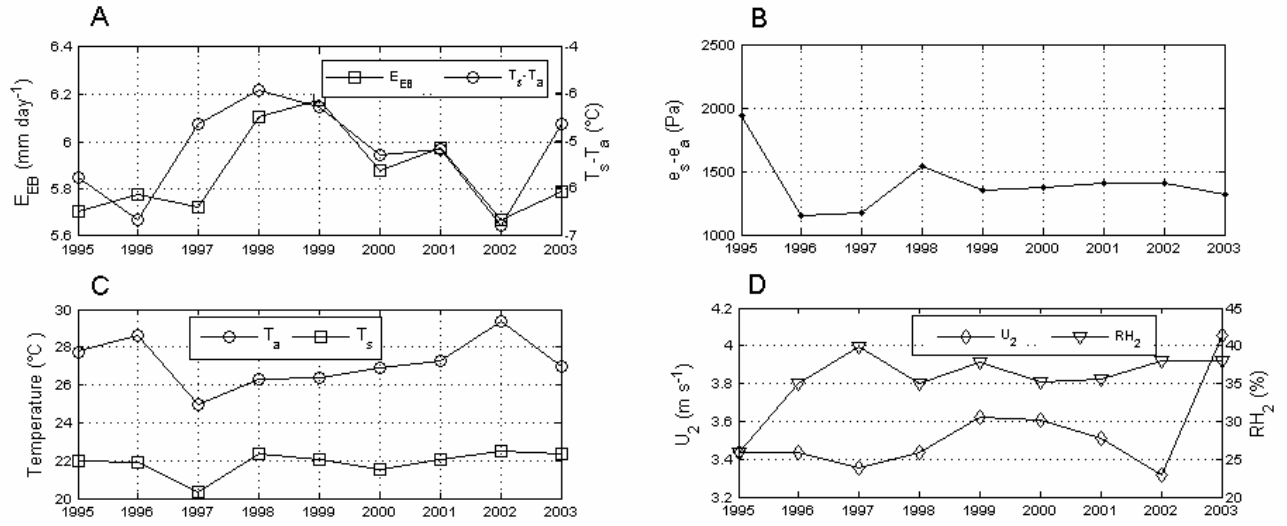


**Fig. 5:** Interannual variability in the atmospheric and limnological variables for Lake Nasser during 1995-2004. Quantities include (A) $E_{EB}$ and $T_0$-$T_a$, (B) $e_0$-$e_a$, (C) $T_0$ and $T_a$, and (D) $RH_2$ and $U_2$

significantly modified the underlying seasonal variability, indicating that one cannot assume that lake evaporation for a particular year will simply follow an 'average' seasonal cycle.

Given the significant evaporation variability on each of these three timescales, the remainder of the analysis was partitioned into three sections: (1) seasonality, (2) interannual variability, and (3) short-term variations. Appropriate averaging was performed to highlight the various timescales. In order to simplify the analysis, we have sampled the various 14-day running mean time series once every 14-days to create a biweekly dataset that is non-overlapping in time. The 26 biweekly periods (listed in Table 1) are the same, year to year. The evaporation estimates in these periods show important uncertaintied due to negative BR values in spring and summer season every year.

**Seasonal variability:** Fig. 3 and Table 1 show the mean seasonal energy budget of Lake Nasser (average over the number of years listed in table 1). $Q_n$ had a relatively wide and flatter seasonal distribution, reaching a maximum of 220.4 W m$^{-2}$ during the period 2-16 June and dropped off thereafter during the months December and January every year. $Q_v$ had a very well defined and relatively narrow peak around the flood season, which maximized roughly three months later to $Q_n$ and droped off significantly during the

**Table - 1:** List of 26 biweekly energy budget periods selected for study and the number of years with available data. Also shown are the mean energy budget components for each biweekly period as well as the overall 26 week mean and standard deviation. Start and end dates for each biweekly period are weighted by 50% to produce a centered, 14 day average. Variables are defined in equations 1,2, 7 and 8.

| Period | Start | End | No. of years | Season name | $E_{EB}$ (W $m^{-2}$) | $Q_v$ (W $m^{-2}$) | $Q_x$(W $m^{-2}$) | $Q_n$(W $m^{-2}$) | BR |
|---|---|---|---|---|---|---|---|---|---|
| 1 | 15-Dec | 29-Dec | 9 | Winter time | 121.22 | 0.812 | -76.908 | 57.652 | 0.08 |
| 2 | 14-Jan | 28-Jan | 9 | | 122.612 | -4.06 | -54.056 | 86.536 | 0.08 |
| 3 | 28-Jan | 11-Feb | 10 | | 123.888 | -6.38 | -33.64 | 102.66 | 0.02 |
| 4 | 11-Feb | 25-Feb | 10 | | 119.132 | -9.164 | -18.792 | 115.536 | 0.02 |
| 5 | 25-Feb | 10-Mar | 10 | | 114.608 | -9.976 | 13.688 | 132.588 | -0.08 |
| 6 | 10-Mar | 24-Mar | 10 | | 148.944 | -12.296 | -8.816 | 146.276 | -0.07 |
| 7 | 24-Mar | 7-Apr | 10 | Spring time | 136.416 | -11.252 | 21.344 | 166.228 | -0.06 |
| 8 | 7-Apr | 21-Apr | 10 | | 163.328 | -9.164 | 20.88 | 188.5 | -0.06 |
| 9 | 21-Apr | 5-May | 10 | | 158.456 | -9.512 | 43.5 | 198.94 | -0.10 |
| 10 | 5-May | 19-May | 10 | | 194.532 | -13.108 | 17.516 | 210.54 | -0.11 |
| 11 | 19-May | 2-Jun | 10 | | 201.26 | -24.244 | 8.584 | 205.784 | -0.16 |
| 12 | 2-Jun | 16-Jun | 10 | | 143.26 | -29.696 | 68.788 | 220.632 | -0.19 |
| 13 | 16-Jun | 30-Jun | 10 | Summer time | 153.932 | -28.884 | 33.292 | 208.568 | -0.09 |
| 14 | 30-Jun | 14-Jul | 10 | | 183.744 | -16.356 | 21.344 | 210.192 | -0.11 |
| 15 | 14-Jul | 28-Jul | 9 | | 208.568 | 14.5 | 23.2 | 208.452 | -0.08 |
| 16 | 28-Jul | 11-Aug | 9 | | 238.96 | 88.508 | 63.684 | 203.232 | -0.09 |
| 17 | 11-Aug | 25-Aug | 9 | | 236.988 | 142.332 | 100.34 | 182.352 | -0.09 |
| 18 | 25-Aug | 8-Sep | 9 | | 241.976 | 151.728 | 92.916 | 169.36 | -0.10 |
| 19 | 8-Sep | 22-Sep | 9 | | 221.792 | 108.46 | 72.732 | 167.736 | -0.11 |
| 20 | 22-Sep | 6-Oct | 9 | Autumn time | 208.8 | 62.06 | 19.952 | 158.92 | -0.08 |
| 21 | 6-Oct | 20-Oct | 9 | | 197.548 | 38.976 | -25.172 | 131.544 | -0.04 |
| 22 | 20-Oct | 3-Nov | 9 | | 177.132 | 22.62 | -60.32 | 98.948 | -0.01 |
| 23 | 3-Nov | 17-Nov | 9 | | 132.936 | 11.948 | -50.344 | 77.14 | 0.01 |
| 24 | 17-Nov | 1-Dec | 9 | | 125.28 | 3.248 | -66.352 | 67.628 | 0.06 |
| 25 | 1-Dec | 15-Dec | 9 | | 156.136 | 2.204 | -107.996 | 72.268 | 0.14 |
| 26 | 1-Jan | 14-Jan | 9 | | 102.08 | -3.248 | -57.188 | 64.612 | 0.13 |
| Mean | | | | | 167.4 | 17.7 | 2.44 | 148.2 | -0.04 |
| Standard deviation | | | | | 42.93 | 50.78 | 54.77 | 54.99 | 0.083 |

months December and January. Lake Nasser is one of the largest artificial lakes on the world, situated in a hot and extremely arid climate, occasionally receiving a large amount of stream discharge from the upper Nile basin catchments. The annual average inflow to Lake Nasser during the period 1900-2002 is estimated to be $86x10^3$ million $m^3$, of which 60% comes during the flood season (August-October). This massive inflow that comes annually leads to the maximum value of $Q_v$ due to the very warm lake at the time of its peak more than the remaining year, during which a lot of water is being lost by evaporation. In addition, the annual outflow from the lake was estimated to be $55.5x10^3$ million $m^3$. The peak outflow happens during the rice-planting season while the inflow to the lake is considered low during this period. This means that the river inflow helps to cool down the lake. Accounting for the previous consideration, $Q_v$ was a very significant term in the energy budget of Lake Nasser. It played an important role in the Lake Nasser reservoir management. The absence of the $Q_v$ term would give higher evaporation estimation during the recession time and lower evaporation estimation during the high inflow period. In Fig. 3 the $Q_v$ term was negative during the months February to July, which gave lower evaporation estimation and positive during August to January, which gave higher evaporation estimation.

Also the $Q_x$ term exhibited seasonal behavior and simply showed a general increase in cooling as the season progresses. In December, the sensible heat flux equals nearly 1/3 that of evaporation, and sensible cooling rates roughly twice that in spring (Table 1).The seasonal change in sensible cooling was associated with a corresponding change in the BR (Table 1). $Q_x$ had a local peak around mid June given that it combined the influences of both radiative and surface heat fluxes (Fig. 2).

Although the energy budget based method is a useful tool for calculating evaporation rates, its utility for understanding the climatic mechanisms controlling evaporation is somewhat limited, particularly for timescales less than a year (Lenters *et al.*, 2005). This is because, in the context of the energy budget, evaporation is a driver (of lake heat storage) as well as a response (to radiation, often with significant time lags). Arguably, a more fundamental driver of lake evaporation is the vapor pressure difference between water and air, which is strongly dependent on factors such as temperature,

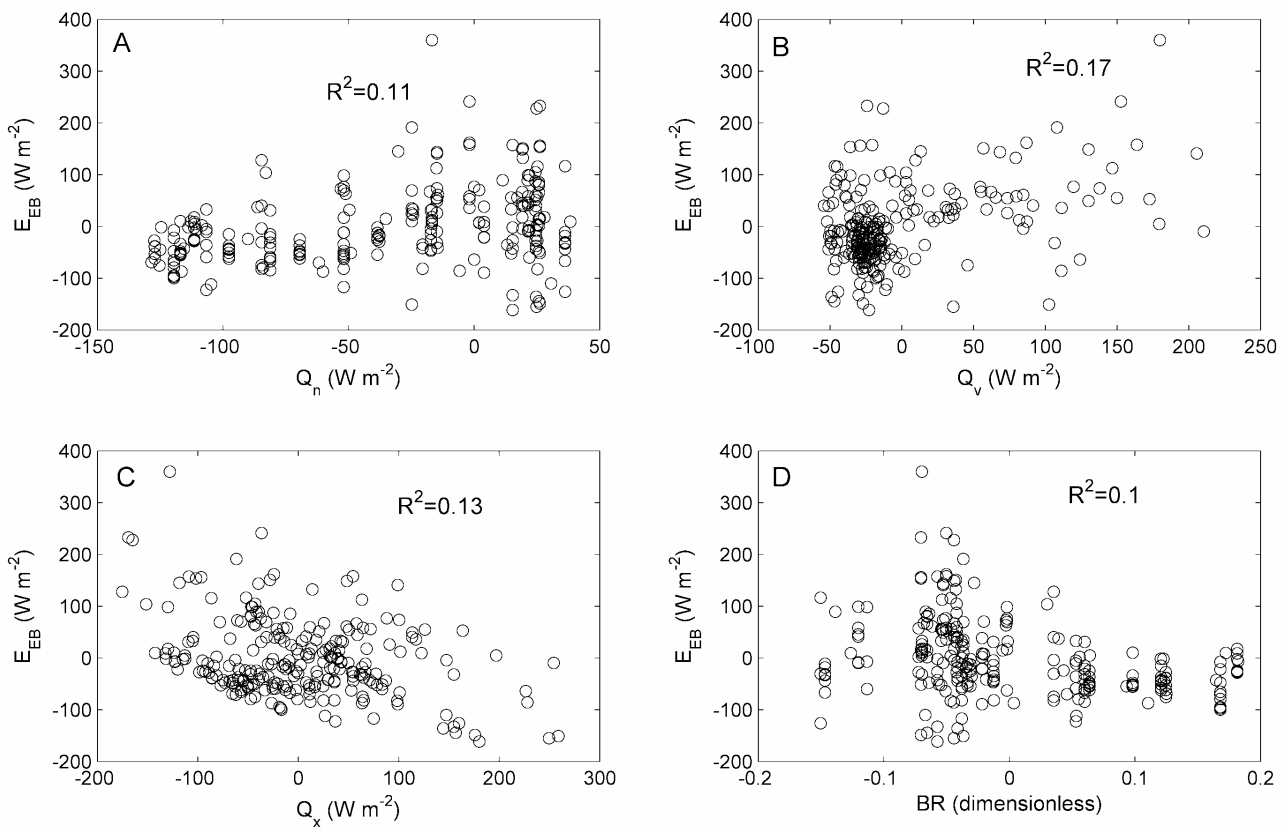


**Fig. 6:** Lake Nasser evaporation rate ($E_{EB}$) vs. (A) $Q_n$, (B) $Q_v$, (C) $Q_x$ and (D) BR. All energy quantities are in W $m^2$. Each dot represents one of the biweekly periods during the 10 years (1995-2004) and are expressed as intraseasonal anomalies (biweekly deviations from the mean seasonal and interannual variability). Also shown are the linear regression lines and associated $R^2$ values

**Table - 2:** Correlation coefficients between Lake Nasser evaporation rate and various energy budget and atmospheric quantities, as a function of timescale

| Timescale | $Q_x$ | $Q_v$ | $Q_n$ | $RH_2$ | $U_2$ | $e_0$-$e_a$ | $T_0$-$T_a$ | BR | $T_0$ | $T_a$ |
|---|---|---|---|---|---|---|---|---|---|---|
| Seasonal | 0.65 | 0.73 | 0.60 | -0.74 | -0.04 | 0.83 | -0.64 | -0.58 | 0.85 | 0.84 |
| Interannual | 0.27 | 0.85 | -0.35 | 0.15 | 0.17 | -0.01 | 0.69 | 0.35 | 0.24 | -0.41 |
| Interseasonal | 0.48 | 0.73 | 0.55 | -0.52 | 0.01 | 0.70 | -0.49 | -0.55 | 0.92 | 0.81 |
| Winter | -0.78 | 0.04 | -0.21 | -0.10 | -0.01 | 0.16 | 0.44 | 0.22 | -0.51 | -0.37 |
| Spring | -0.98 | -0.36 | 0.52 | -0.01 | -0.36 | 0.31 | 0.45 | 0.16 | -0.17 | -0.46 |
| Summer | -0.24 | 0.62 | 0.69 | 0.45 | 0.13 | -0.40 | 0.21 | 0.41 | 0.10 | -0.17 |
| Autumn | -0.80 | 0.53 | -0.14 | -0.26 | -0.01 | 0.26 | 0.05 | 0.85 | 0.27 | 0.06 |

**Table - 3:** Year to year average evaporation, standard deviation, coefficient of variation (CV) and percentage of evaporation variation of the average evaporation rate in biweekly mean evaporation

| Year | 1995 | 1996 | 1997 | 1998 | 1999 | 2000 | 2001 | 2002 | 2003 |
|---|---|---|---|---|---|---|---|---|---|
| Average evaporation (mm $d^{-1}$) | 5.70 | 5.78 | 5.72 | 6.11 | 6.20 | 5.87 | 5.97 | 5.67 | 5.79 |
| Standard deviation (mm $d^{-1}$) | 2.30 | 2.82 | 2.20 | 3.99 | 3.06 | 2.79 | 2.43 | 2.56 | 1.45 |
| Coefficient of variation (CV) | 40.90 | 48.80 | 38.50 | 65.30 | 49.48 | 47.50 | 40.64 | 45.20 | 25.00 |
| % variation | 2.33 | 1.05 | 1.98 | 4.60 | 5.77 | 0.60 | 2.30 | 3.00 | 0.90 |

humidity and wind speed. Fig. 4 illustrates a number of these climatic influences for Lake Nasser, focusing on the average seasonal cycle (1995-2004 in most cases; Table 1).

The distinct seasonal variation in Lake Nasser evaporation rates (Fig. 4A) is largely explained by similar variations in lake surface temperature (Fig. 4D), which reached its maximum during the same 2 week period. $T_a$ followed a similar curve (Fig. 4D) and was 9°C hotter than the $T_0$ (Fig. 4D). This temperature difference was greatest at the end of autumn and the beginning of the summer and was partly responsible for the changes in sensible heat flux and BR (Table 1). The BR value decreased from around 0.13 in January to its most negative value of -0.19 by early June (Fig. 4F).

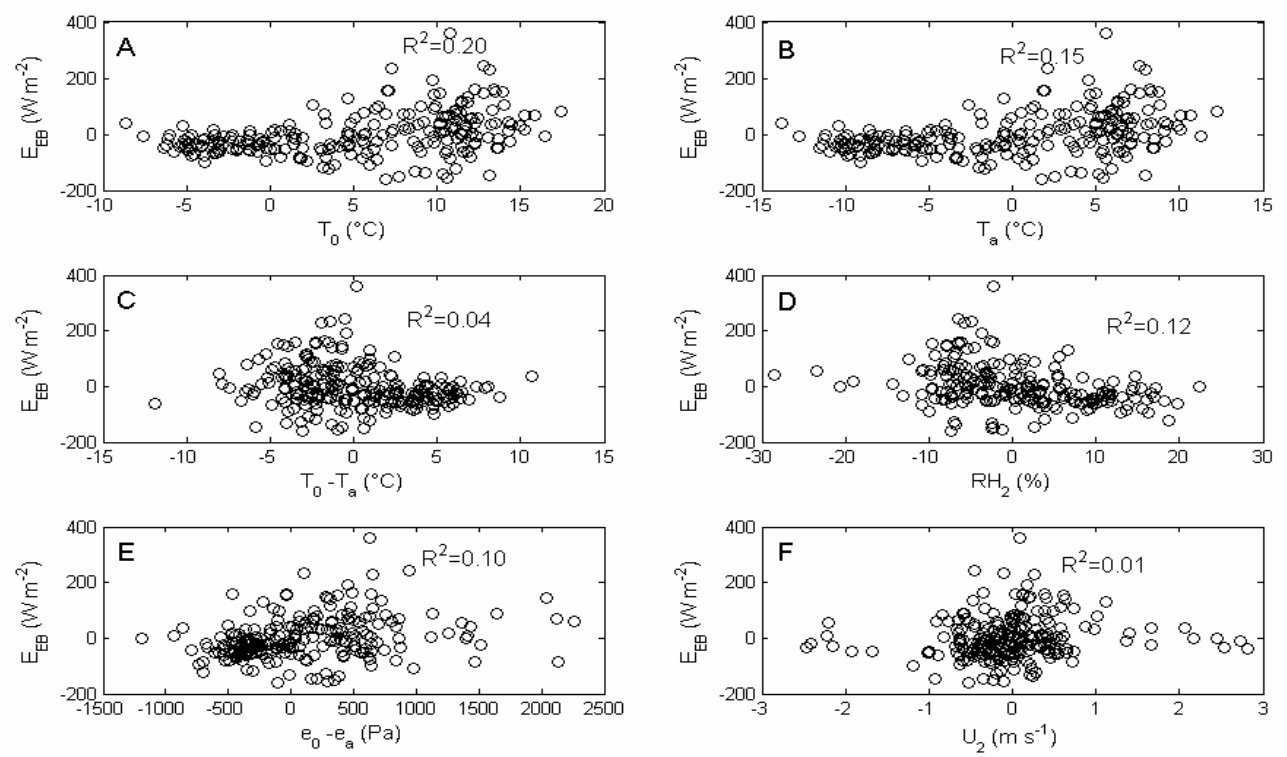


**Fig. 7:** Lake Nasser evaporation rate ($E_{EB}$, in W m$^2$) vs. (A) $T_0$, (B) $T_a$, (C) $T_0$-$T_a$, (D) $RH_2$, (E) $e_0$-$e_a$ and (F) $U_2$. All quantities are expressed as intraseasonal anomalies (biweekly deviations from the mean seasonal and interannual variability). Each dot represents one of the biweekly periods during the 10 years (1995-2004). Also shown are the linear regression lines and associated $R^2$ values

**Table - 4:** Interannual variability in the Lake Nasser energy budget. Also shown are the long-term mean and interannual standard deviation. Variables are defined in equations 1,2, 7 and 8

| Year | $E_{EB}$ (W m$^{-2}$) | $Q_v$ (W m$^{-2}$) | $Q_x$ (W m$^{-2}$) | $Q_n$ (W m$^{-2}$) | BR |
|---|---|---|---|---|---|
| 1995 | 162.052 | 10.092 | 7.076 | 153.932 | -0.05 |
| 1996 | 164.256 | 24.128 | 11.484 | 148.248 | -0.04 |
| 1997 | 162.748 | 12.876 | 1.044 | 148.248 | -0.04 |
| 1998 | 173.536 | 31.088 | 8.584 | 148.132 | -0.04 |
| 1999 | 175.508 | 28.42 | 4.408 | 148.248 | -0.04 |
| 2000 | 167.04 | 14.732 | -1.044 | 148.48 | -0.04 |
| 2001 | 169.824 | 18.676 | 0.812 | 148.248 | -0.04 |
| 2002 | 161.008 | 5.452 | -4.756 | 148.248 | -0.04 |
| 2003 | 164.604 | 15.66 | 2.32 | 148.248 | -0.04 |
| Mean | 166.692 | 17.864 | 3.364 | 148.828 | -0.04 |
| Standard deviation | 5.22 | 8.468 | 5.104 | 1.856 | 0.004 |

Through the non-linear effect of temperature on vapor pressure, seasonal changes in water and air temperature led to a vapor pressure difference curve of which the general trend was similar to that of the calculated evaporation rate (Fig. 4A,B). Intraseasonal variations in evaporation values, such as the low values in late May and October, did not reflect the values of the lake-air temperature difference (Fig. 4A), but reflected the values of the $Q_x$ and $Q_v$ terms (Fig. 3). This led to the conclusion that the simpler traditional method that contains a wind speed term (mass transfer) or the method that makes use of only $T_a$ (the Papadakis method) might provide unadequate estimates of Lake Nasser evaporation rates. The correspondence between evaporation and vapor pressure difference also helps to corroborate the results of the more rigorous energy budget method.

In addition to temperature, other meteorological factors likely to affect seasonal evaporation rates include relative humidity ($RH_2$) and wind speed ($U_2$) at 2 m above the lake surface. Average variations in $RH_2$ over Lake Nasser (Fig. 4E) showed a decrease from roughly 50% yearly in January to around 30% by end of June. Although these seasonal changes are rather minor compared to temperature, they were large enough to produce noticeable differences in evaporation rate. For example, if the $RH_2$ during the first 2 week period would be decreased from the observed value

(50%) to a mid-season value (30%), the lake-air vapor pressure difference $e_0$-$e_a$ would be increased by 400%. This suggests that $RH_2$ variations moderate the temperature-induced seasonality in evaporation by raising evaporation rates during summer and lowering them during springtime and fall.

Average wind speeds over Lake Nasser (Fig. 4C) showed a pattern of low wind speeds during the winter, spring and summer time and relatively higher values during the autumn time. As a result, inclusion of wind speed as a linear term in the vapor pressure difference curve (Fig. 4B) led to a less favorable comparison with the energy budget derived evaporation rates (Fig. 4A). This unexpected result suggests that, on seasonal timescales, it may not be appropriate to include wind speed as a linear term in the mass transfer evaporation estimates for Lake Nasser. A possible explanation for this is that the lower boundary layer may be sufficiently well mixed for wind speeds of 3-4 m $s^{-1}$, such that the small seasonal variations (Fig. 4C) have little, if any, impact on evaporation.

**Interannual variability:** Lake Nasser experienced significant interannual variations in evaporation (Fig. 2). This was also evident in the interannual coefficient of variation (CV) in evaporation for each of the 10 energy budget periods (Table 3). Typical year-to-year variations in 14-day mean evaporation ranged from 0.6 to 5.77% of the average evaporation rate and was usually within the maximum error bounds. Large interannual variability occured during 5–19 May (CV =66%). The minimum interannual variation occured normally at winter time (11.7% during 14-28 January). Year-to-year changes in the average evaporation were moderate (Table 3). Despite these moderate changes, the coefficient of variation changes relatively large from year to year (25-65.30%). This was due to the strong short-term variations in evaporation (Fig. 2).

To assess interannual variations in winter, spring, summer and autumn averages, 12 and 14-week means were created for each seasonby averaging the energy budget and meteorological variables over six and seven energy budget periods: from 15th December to 24th March (winter time, Table 1), from 24th March to 16th June (spring time, Table 1), from 16th June to 22th September (summer time, Table 1), and from 22th September to 15th December (autumn time, Table 1). Average energy budget components for each year are shown in Table 4 along with the 10 year mean and standard deviations. Interannual variations in BR, $Q_n$, $Q_x$ and $Q_v$ (Table 4) were considerably smaller than the corresponding seasonal variations (Table 1). This was primarily because seasonal variations in temperature and solar radiation were significantly larger than year-to-year variations (particularly when averaged over a seasonal period). The interannual standard deviation of evaporation rate (Table 4) was also much less than that of the seasonal cycle (Table 1). In fact, year-to-year variations in $E_{EB}$, $Q_n$ and BR were roughly 2.5, 1 and 5% of their mean values, respectively. Whereas the year-to-year variation in $Q_x$ and $Q_v$ was subjected to significant large variation (92 and 40% of their mean values, respectively). This indicates that the interannual changes in $E_{EB}$ were strongly influenced by $Q_x$ and $Q_v$. Generally the interannual changes in the energy budget, though smaller than seasonal variations, were not insignificant.

Table 4 shows slightly change in the energy budget year-to-year. During the years 1998 and 1999, evaporation rates were relatively higher. This change was due to the high floods in 1998 and 1999. Remaining year-to-year variations were less conclusive, since they fall within the estimated measurement uncertainty. As with the seasonal variability, we now examine other climatic variables related to the interannual changes in lake evaporation. These are shown in Fig. 5 as mean quantities. $Q_n$ was relatively higher in 1995 (Fig. 5B). The remaining years were almost constant. This was supported by the relatively small year-to-year changes in $Q_x$ and $Q_v$ (Fig. 5C). A comparison of Fig. 5B-D with the annual $E_{EB}$ (Fig. 5A) revealed that neither lake $T_0$, $T_a$, $RH_2$, $Q_n$, $Q_x$, $e_0$-$e_a$ nor $U_2$ were (by themselves) strongly related to changes in evaporation on interannual timescales (Table 2). Table 2 reveals that both $Q_v$ and $T_0$-$T_a$ were relatively strong related to changes in evaporation.

Some correspondence, however, is evident. For example, the decrease in evaporation from 1996 to 1997 (Fig. 5A) is associated with the largest one-year drop in water and air temperatures ($T_0$ and $T_a$), net energy advected and the change in the stored energy ($Q_v$ and $Q_x$) during the 10-year period (Fig. 5C-D). The same type of changed happened from 1997 to 1998 where the evaporation suddenly increased due to increases in the same parameters ($T_0$, $T_a$, $Q_v$ and $Q_x$). From 2001 to 2002, a strong drop in the evaporation occurred due to increase in the lake surface and air temperatures. This drop was mainly associated with the drop in the net advected energy and the change in stored energy.

**Short-term variations:** To analyze the short-term, intraseasonal variations in evaporation rate, discrepancies (anomalies) were calculated for each14-day period. This was done by first removing the average seasonal cycle (Fig. 4A) from the raw time series (Fig. 2, sampled every 14 days). Next, interannual variations were removed by subtracting the annual anomalies (Fig. 5A; $E_{EB}$). The same procedure was then used to calculate intraseasonal anomalies for other energy budget and climatic variables. The standard deviation of intraseasonal evaporation anomalies was 37.4 W $m^{-2}$, which was smaller than the seasonal variability (Table 1) but greatly larger than the interannual standard deviation (Table 4). Net radiation anomalies rather followed a beta distribution (not shown) with a standard deviation of 48.6 W $m^{-2}$ (much larger than the interannual variability; Table 4). Anomalous heat storage showed a much larger standard deviation (52.2 W $m^{-2}$) since it combined the influences of both radiative and surface heat fluxes. This value was considerably larger than the interannual variability (Table 4), but still lesser than the seasonal standard deviation (Table

2). Bowen ratio anomalies were normally distributed with a standard deviation of 0.064 (comparable to the interannual variability).The covariances of the energy budget components are illustrated in Fig. 6. This figure showed that the various energy components and the BR parameter were essentially moderately correlated with the evaporation rate (Fig. 6A,B and C), indicating that short-term variations in Lake Nasser evaporation are weakly driven by the $Q_n$, $Q_x$, $Q_v$ and BR anomalies during the same 14-day period. Evaporation was negatively correlated with lake heat storage (Fig. 6C) and, therefore, was an important driver of intraseasonal lake temperature changes. It was also worth noting that intraseasonal variations in BR showed essentially no relationship to changes in evaporation (Table 2).

Connections between short-term variations in evaporation and local climate are examined in Fig. 7. $T_0$ anomalies were not significantly related to intraseasonal changes in evaporation (Fig. 7A). This was primarily because $T_0$ increases are usually accompanied by higher $T_a$ as well, which reduced the $e_0$-$e_a$. In fact, the effects of $T_a$ on absolute humidity outweighed the impact on $T_0$, resulting in a strong positive (and statistically significant) relationship between $T_a$ and $E_{EB}$ (Fig. 7B; Table 2). Combined with the effects of water temperature, this led to a relatively strong negative correlation between $E_{EB}$ and the lake-air temperature difference $T_0$-$T_a$ (Fig. 7C; Table 2). Unlike the interannual variations, the correlation was positive. This implied that, on 14-day timescales, vapor pressure effects on evaporation dominate the negative feedback of evaporative cooling. It was also possible that the connection between $E_{EB}$ and the $T_0$-$T_a$ was due, in part, to the effects of atmospheric stability (*i.e.* higher $T_0$-$T_a$, greater instability, higher evaporation).

$RH_2$ exhibited a significant, negative correlation with intraseasonal evaporation anomalies (Fig. 7D, Table 2). This is physically intuitive and lends some confidence to the otherwise uncertain $RH_2$ measurements. When temperature and humidity were combined into vapor pressure anomalies, the resulting relationship with evaporation was strongly positive (Fig. 7E, Table 2). This verifies the vapor pressure connection first seen in Fig. 4A and B and indicates that a mass transfer approximation is suitable for intraseasonal timescales (as it is also for seasonal timescales, but not interannual). In contrast to the seasonal and interannual timescales, short-term variations in wind speed were moderately correlated with evaporation (Fig. 7F), as was also found by Blanken et al. (2000) for Great Slave Lake. However, including it with vapor pressure in the mass transfer formula ($U_2(e_0 - e_a)$, Table 2) led to little improvement in the overall relationship.

This study has provided a comprehensive 10-year analysis of seasonal, intraseasonal, and interannual variations in lake evaporation using the BREB method. The long-term mean evaporation rate for Lake Nasser is found to be 5.83 mm $day^{-1}$ (averaged over all available 14-day periods), with a coefficient of variation of 63%.

The lake evaporation is highly variable on a wide range of timescales. This is particularly true for the seasonal timescale, which exhibits an average range in evaporation from 4.4 mm $day^{-1}$ in winter to 6.0 mm $day^{-1}$ in spring, 7.5 mm $day^{-1}$ in summer and 5.7 mm $day^{-1}$ in autumn.

Even though the seasonal cycle is clearly evident when evaporation rates are averaged over all available years, it is much more poorly defined for individual years because of significant intraseasonal variations. The most important individual climatic influence on intraseasonal variations in evaporation is lake surface temperature. This was followed by air temperature, vapor pressure difference, relative humidity, lake–air temperature difference and wind speed.

Year-to-year changes in mean annual evaporation, while generally smaller than the seasonal and intraseasonal variations, are by no means negligible.

An important result of this study is that the effectiveness of the mass transfer formulation depends strongly on the timescale being considered as well as the characteristics of the local wind field. In the Lake Nasser area, seasonal temperature variations are large, resulting in a robust relationship between evaporation and vapor pressure difference on seasonal timescales. The relationship is weaker for the intraseasonal and interannual time scales, for which temperature variations are considerably reduced. With the exception of Ikebuchi *et al.* (1988), other studies have also indicated difficulties in applying the mass transfer formula over a wide range of timescales (*e.g.* Winter, 1981; Sturrock *et al*., 1992; Sacks *et al*., 1994).

## References

Allen, R., L. Pereira, D. Raes and M. Smith: Crop evapotranspiration. Guidelines for computing crop water requirements. FAO Irrigation and Drainage Paper 56. FAO-Food and Agriculture Organization of the United Nations, Rome, M-56 ISBN 92-5-104219-5 (1998), http://www.fao.org/docrep/x0490e/x0490E00.htm.

Blanken, P.D., W.R. Rouse, A.D. Culf, C. Spence, L.D. Boudreau, J.N. Jasper, B. Kochtubajda, W.M. Scertzer, P. Marsh and D. Verseghy: Eddy covariance measurements of evaporation from Great Slave lake, Northwest Territories, Canada. *Water Res. Res.*, **36**, 1069-1077 (2000).

Elsawwaf, M., P. Willems, A. Pagno and J. Berlamont: Evaporation estimates from Nasser lake, Egypt, based on three floating station and Bowen ratio energy budget. *Theor. Appl. Climatol.*, **100**, 439-465 (2010a).

Elsawwaf, M., P. Willems and J. Feyen: Assessment of the sensitivity and prediction uncertainty of evaporation models applied to Nasser lake, Egypt. *J. Hydrology*, **395**, 10-22 (2010b).

Ikebuchi, S., M. Seki and A. Ohtoh: Evaporation from lake Biwa. *J. Hydrol.,* **102**, 427-449 (1988).

Lenters, J.D., T.K. Kratz and C.J. Bowser: Effects of climate variability on lake evaporation: Results from a long-term energy budget study of sparkling lake, northern Wisconsin (USA). *J. Hydrol.,* **308**, 168-195 (2005).

Lee, T.M. and A. Swancar: Influence of evaporation, ground water, and uncertainty in the hydrologic budget of Lake Lucerne, a seepage lake in Polk County, Florida. Water-Supply Paper 2439, US Geological Survey (1997).